Supernova Neutrinos: The Accretion Disk Scenario

G. C. McLaughlin[1] and R. Surman[2]
[1] *Department of Physics, North Carolina State University, Raleigh, North Carolina 27695-8202.*
[2] *Department of Physics and Astronomy, Union College, Schenectady, NY 12308.*

(Dated: February 5, 2008)

Neutrinos from core collapse supernovae can be emitted from a rapidly accreting disk surrounding a black hole, instead of the canonical proto-neutron star. For Galactic events, detector count rates are considerable and in fact can be in the thousands for Super-Kamiokande. The rate of occurrence of these accreting disks in the Galaxy is predicted to be on the order of $\sim 10^{-5}\,\mathrm{yr}^{-1}$, yet there is little observational evidence to provide an upper limit on their formation rate. It would therefore be useful to discriminate between neutrinos which have been produced in a proto-neutron star and those which have been produced accretion disks. In order to distinguish between the two scenarios, either the time profile of the neutrino luminosity or the relative fluxes of different neutrino flavors may be considered. There are some signals that would clearly point to one scenario or the other.

PACS numbers: 26.50.+x,13.15.+g,97.60.Bw

Recent advances in the theory of gamma ray bursts (GRBs) have pointed to rapidly accreting disks surrounding black holes (AD-BH) because this configuration is a natural one for producing massive energy generation. Simulations of neutron star mergers and core collapse supernovae have indeed found that under certain conditions, these disks can form [1, 2, 3]. Spectra from X-ray afterglows of long duration bursts have indicated that the bursts are associated with Type Ib/Ic supernovae, suggesting massive stellar core collapse as the origin. The rate of gamma ray bursts in the galactic region is estimated to be approximately $10^{-5}\,\mathrm{yr}^{-1}$ with approximately 2/3 of these being long duration events [4]. This is roughly 0.1% of the core collapse supernova rate. Disks which produce enough energy for a burst must have fairly high accretion rates in the range of 0.1 $M_\odot/\,\mathrm{s}$ to 1.0 $M_\odot/\,\mathrm{s}$. Observations of short bursts suggest that they are associated with compact object mergers, neutron star - neutron star, or black hole-neutron star [5].

Hypernovae are very energetic core collapse supernova. The rate of Type Ic supernovae in an average galaxy is about $10^{-3}\,\mathrm{yr}^{-1}$, whereas the inferred hypernova rate is about $10^{-5}\,\mathrm{yr}^{-1}$ [4] . A limited data set of Type Ic hypernovae and supernovae shows that supernovae which come from progenitors above $\sim 20M_\odot$ show evidence for two branches with a few stars at high energy $\sim 10^{52}$ ergs, and one at low energy $\sim 10^{50}$ ergs [6]. One can speculate that the more luminous events are produced by an accretion disk and the less luminous event is not.

It would be useful to translate these limits on hypernovae and gamma ray bursts into limits on the AD-BH formation rate. Not every AD-BH may make a hypernova or GRB. An observationally based upper limit can be made from the ratio of black holes to neutron stars. In the case of low-mass x-ray transients the observations will support turning every star above $\sim 20\mathrm{M}_\odot$ into a black hole [7], producing a rate of 10% or even greater.

In this paper we point out that the next Galactic supernova may produce neutrinos in an accretion disk, not in a proto-neutron star. Even if the supernova light curve is observed, it would be difficult to use this to determine whether a PNS or an AD-BH is formed at the core. In this paper we show that the emitted neutrinos may be used to immediately and directly make this distinction.

Detectors that will observe neutrinos from the next galactic supernova are currently Super-Kamiokande [8], KamLAND [9], MiniBooNE [10], SNO [11] and the future Borexino [12] . A proto-neutron star event will produce 1000s of events in SuperK, and 100s in KamLAND and MiniBooNE. At least one count from an AD-BH supernova may occur in SuperKamiokande even if the event is 3 Mpc away[13].

To estimate the neutrino signal, we first examine the disks from which they are emitted. Neutrinos in accretion disks are produced primarily in inverse beta decay events. For sufficiently rapidly accreting disks the center of the disk has high enough temperature that the neutrinos become trapped. Fig. 1 shows the surfaces of last scattering for the neutrinos in the PNS and the AD. Fig 1b is based on the calculations of [14] for an AD of $\dot{M} = 1.0 M_\odot/\,\mathrm{s}$, and black hole spin parameter a= 0, while Fig. 1a was estimated from the protoneutron star temperature and density profile of Ref. [15]. For a disk which accretes at a rate 0.1 $M_\odot/\,\mathrm{s}$, the neutrinos are only barely trapped.

If one wishes to detect neutrinos from an AD-BH supernova, the total energy emitted in the form of neutrinos is clearly important. For the PNS, analyses are often done by taking $3\times10^{53}\,\mathrm{erg}$ of gravitational binding energy liberated in the collapse and dividing it equally between six species, three flavors of neutrinos and three of antineutrino. In the case of the AD-BH, gravitational binding energy is released as material spirals in from the outer edges of the disk but only some of that is released in the

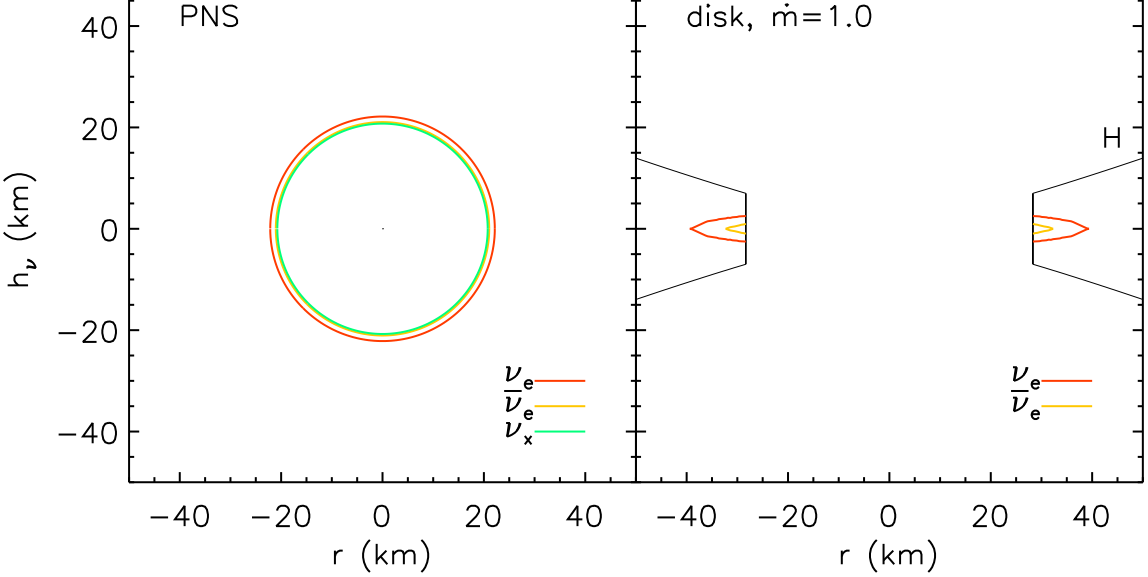

FIG. 1: Shows the neutrino surfaces for a proto-neutron star and a 1 $M_\odot$/s accretion disk.

form of neutrinos. The gravitational binding energy released, given a 3 $M_\odot$ black hole, is $9\,(M/M_\odot) \times 10^{53}$ergs, where M is the mass of material processed by the disk. When the neutrinos are not trapped the rate of energy loss is determined by the rate at which neutrinos can be produced through inverse beta processes. When neutrinos are trapped it is determined by the time it takes the neutrinos to scatter out of the trapped region. We find that roughly 20% of this gravitational binding energy is released in the form of neutrinos for disks of 1.0 $M_\odot$/ s and 5% in the case of 0.1 $M_\odot$/ s.

The timescale for neutrino emission through the proto-neutron star is about 10 s, with an exponentially decaying luminosity so that most of the neutrinos are emitted in the first three seconds. If an accretion disk is steady state, the neutrino luminosity will not fall off but will be approximately constant. For example, for a 0.01 $M_\odot$ / s disk which processes 1 $M_\odot$, the neutrino emission will be spread over 100 s, although deviations from steady state will likely occur. The observed time profile of the neutrinos may be used as a constraint.

The energy spectra of the emitted neutrinos will determine the flux averaged cross sections in supernova neutrino detectors. Over the trapping surface in the $\dot{M} = 1 M_\odot$/s AD, the energies are in the range of $\langle E_{\nu_e} \rangle \sim 13\,\mathrm{MeV}$ to $\langle E_{\nu_e} \rangle \sim 14\,\mathrm{MeV}$ and $\langle E_{\bar{\nu}_e} \rangle \sim 16\,\mathrm{MeV}$ to $\langle E_{\bar{\nu}_e} \rangle \sim 18\,\mathrm{MeV}$ [14] . There is relatively little emission due to μ and τ type neutrinos in such disks although for faster accretion rates such as 10 $M_\odot/s$, μ and τ neutrinos are not only produced but also become trapped. In more slowly rotating, optically thin disks, the average energy of the neutrinos comes close to tracking the average thermal energy of the electrons and positrons.

As can be seen from Fig. 2, the spectra of the ν_e and $\bar{\nu}_e$ are similar in the PNS and AD-BH cases. The muon and tau types however, are quite different, suggesting that a detection of the neutrinos by flavor will give a clear signature for one scenario or the other. However, neutrino flavor transformation must be taken into account when translating the flavors of emitted spectra to the flavors that will be measured at the detector.

In both the PNS and AD-BH, the neutrinos are emitted from a place of relatively high density, where they are matter suppressed and essentially coincident with matter eigenstates. As the neutrinos proceed to the outer edges of the star, which is at relatively low density, they pass through two potential resonances regions and emerge as mass eigenstates, see e.g. [18]. The lower density resonance, at $\sim 10\,\mathrm{g\,cm^{-3}}$, is governed by δm_{12}, and θ_{12} both of which have been measured by solar and reactor neutrino experiments. The higher density transition, at $\sim 10^3\,\mathrm{g\,cm^{-3}}$ is governed by δm_{13} and θ_{13} . The former parameter is known except for a sign (leaving the neutrino mass hierarchy unknown) while the later is constrained by reactor neutrino experiments $\sin^2\theta_{13} < 0.1$ [19]. There is some uncertainty regarding how the neutrinos will behave in these regions due to the unknown hierarchy, θ_{13} and the density profile of the star.

The results of various oscillation scenarios are shown in Table I, where we show the ratio of the total energy flux in all νs to that in ν_e, $\bar{\nu}_e$ and the other four neutrinos as seen at a detector. A total energy flux could be inferred from a signal in the neutral current channel, while the ν_e and $\bar{\nu}_e$ fluxes could be inferred through measurements in the charged current channels. It can be seen from the table that if neutrinos come from a PNS, then the energy flux ratios are relatively similar. The ratios for the AD-BH cases, on the other hand, vary considerably. If ν_es or $\bar{\nu}_e$s encounter the higher resonance adiabatically, then there is a clear signature for the AD-BH scenario because the flux ratios differ by an order of magnitude from the PNS. In almost all other cases, there are still differences between the PNS and AD-BH flux ratios of a factor of two.

To determine the relative fluxes in the different channels, sufficient counts are required. In Fig. 3 we compare events that would occur in SuperKamiokande, for a supernova at 10 kpc, which collapses either to a PNS or to an AD-BH. Estimates of total counts for Super-Kamiokande, KamLAND, SNO (as a model for a ν_e sen-

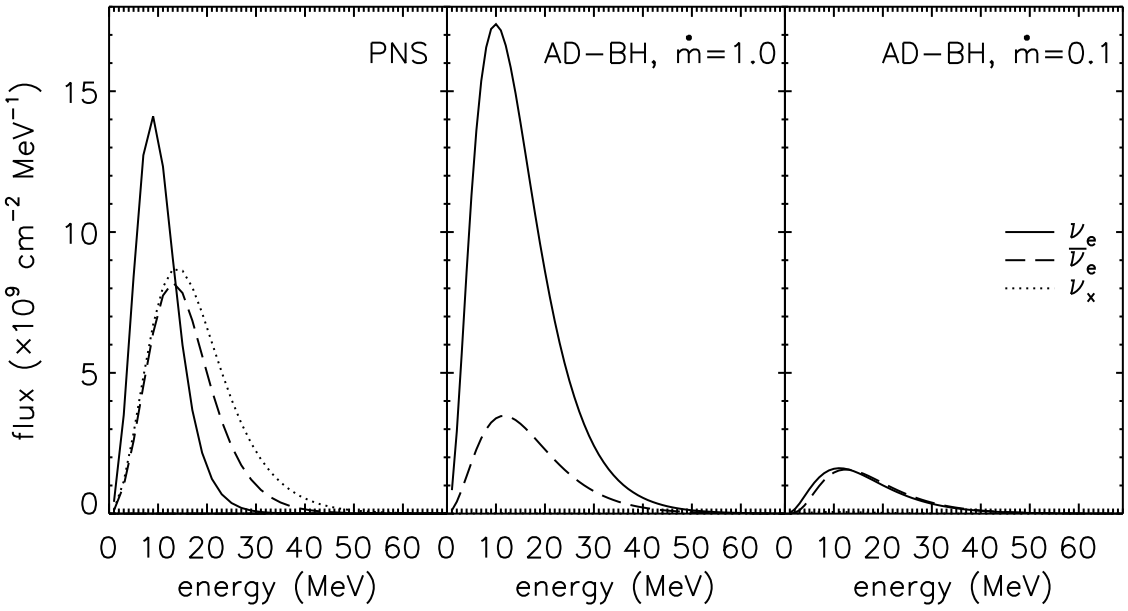

FIG. 2: Shows the neutrino spectra for the PNS and AD-BH, in the absence of oscillations, at a distance of 10 kpc from the center of the object. The AD-BH neutrino spectra were calculated by summing over the entire surface of the disk including both trapped and untrapped regions, as described in [14, 16]. The spectral parameters for the PNS were taken from [17]: $T_{\nu_e} = 2.6$, $\eta = 3.0$, $T_{\bar{\nu}_e} = 4.0$, $\eta = 2.8$, and $T_{\nu_\mu,\nu_\tau} = 5.0$, $\eta = 1.8$, with an energy partition of $L_{\nu_e} : L_{\bar{\nu}_e} : L_{\nu_e}$ of $1 : 1.3 : 7.7$.

sitive detector) and OMNIS are given in Table II. The prospects for making the distinction will depend on which detectors are on line at the time. It is essential to have a good neutral current signal measurement, as this is how the total flux will be measured. It is also vastly preferable to have a way to measure both the ν_e and $\bar{\nu}_e$ flux if one wishes to distinguish between a PNS and an AD-BH.

We have discussed the observational consequences of the next Galactic core collapse event forming at its center an accretion disk surrounding a black hole instead of a proto-neutron star. This type of event will produce significant event rates in currently on-line neutrino detectors, with a time profile that will likely differ from that of the canonical PNS. With a neutral current measurement, it may be possible to determine the origin of core-collapse supernova neutrinos by inferring the ratio of the total energy flux to charged current flux. For the AD-BH scenario this could be as large 1600:1.

This work was supported in part by the Department of Energy, under contract DE-FG02-02ER41216 (GCM), DE-FG05-05ER41398 (RS). and by the National Science Foundation under Grant No. PHY99-7949.

[1] A. MacFadyen and S. E. Woosley, Astrophys. J. **524**, 262 (1999) [arXiv:astro-ph/9810274].
[2] M. Ruffert and H. T. Janka, arXiv:astro-ph/9809280.
[3] S. Rosswog, arXiv:astro-ph/0508138.
[4] P. Podsiadlowski, P. A. Mazzali, K. Nomoto, D. Lazzati and E. Cappellaro, Astrophys. J. **607**, L17 (2004) [arXiv:astro-ph/0403399].
[5] J. Hjorth et al., Nature **437** 859 (2005)
[6] K. Nomoto, K. Maeda, H. Umeda, T. Ohkubo, J. Deng, P. Mazzali, astro-ph/0209064.
[7] C. L. Fryer and V. Kalogera, Astrophys. J. **554**, 548 (2001), [arXiv:astro-ph/9911312.]
[8] Y. Oyama *et al.*, Phys. Rev. Lett. 56, 2604 (1987).
[9] P. Vogel, Prog. Part. Nucl. Phys. **48**, 29 (2002).
[10] M.K. Sharp, J.F. Beacom, J.A. Formaggio, Phys. Rev. D **66**, 013012 (2002).
[11] J. F. Beacom and P. Vogel, Phys. Rev. D **58**, 093012 (1998) [arXiv:hep-ph/9806311].
[12] L. Cadonati, F. P. Calaprice and M. C. Chen, Astropart. Phys. **16**, 361 (2002) [arXiv:hep-ph/0012082].
[13] S. Nagataki and K. Kohri, Prog. Theor. Phys. **108**, 789 (2002) [arXiv:astro-ph/0003066].
[14] R. Surman and G. C. McLaughlin, Astrophys. J. **603**, 611 (2004) [arXiv:astro-ph/0308004].
[15] J. Wilson, private communication
[16] J. P. Kneller, G. C. McLaughlin and R. Surman, J. Phys. G **32**, 443 (2006) [arXiv:astro-ph/0410397].
[17] M. T. Keil, G. G. Raffelt and H. T. Janka, Astrophys. J. **590**, 971 (2003) [arXiv:astro-ph/0208035].
[18] A. S. Dighe and A. Y. Smirnov, Phys. Rev. D **62**, 033007 (2000) [arXiv:hep-ph/9907423].
[19] M. Apollonio *et al.*, Eur. Phys. J. C **27**, 331 (2003).
[20] K. Langanke, P. Vogel and E. Kolbe, Phys. Rev. Lett. **76**, 2629 (1996) [arXiv:nucl-th/9511032].
[21] J. F. Beacom, W. M. Farr and P. Vogel, Phys. Rev. D **66**, 033001 (2002) [arXiv:hep-ph/0205220].
[22] R. N. Boyd, G. C. McLaughlin, A. S. J. Murphy and P. F. Smith, J. Phys. G **29**, 2543 (2003).

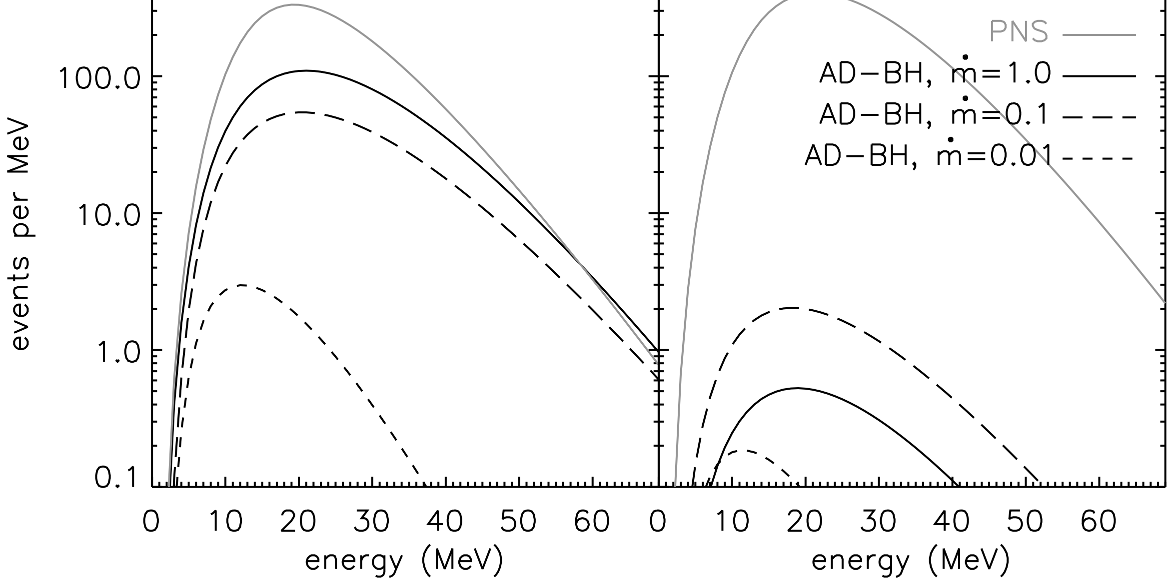

FIG. 3: Comparison between the counts for $\bar{\nu}_e + p \rightarrow e^+ + n$ at SuperKamiokande as a function of positron energy for the two oscillation scenarios. Plotted are the signals from the proto-neutron star and accretion disks of 0.1 $M_\odot$/s to 1.0 $M_\odot$/s. With a normal hierarchy (left panel), a fraction of the neutrinos originally emitted as $\bar{\nu}_e$s are measured as $\bar{\nu}_\mu$ and $\bar{\nu}_\tau$s at the detector. With an inverted hierarchy and an adiabatic θ_{13} resonance (right panel), almost all the neutrinos originally emitted as $\bar{\nu}_e$s are measured as $\bar{\nu}_\mu$ and $\bar{\nu}_\tau$s at the detector. For the PNS this makes relatively little difference as originally emitted $\bar{\nu}_\mu$ and $\bar{\nu}_\tau$s are also converted to $\bar{\nu}_e$.

	Normal Hierarchy H			Normal Hierarchy LA			Normal Hierarchy LNA			Inverted Hierarchy H, LA			Inverted Hierarchy H, LNA		
	$\frac{\text{total}}{\nu_e}$	$\frac{\text{total}}{\bar{\nu}_e}$	$\frac{\text{total}}{\nu_x}$	$\frac{\text{total}}{\nu_e}$	$\frac{\text{total}}{\bar{\nu}_e}$	$\frac{\text{total}}{\nu_x}$	$\frac{\text{total}}{\nu_e}$	$\frac{\text{total}}{\bar{\nu}_e}$	$\frac{\text{total}}{\nu_x}$	$\frac{\text{total}}{\nu_e}$	$\frac{\text{total}}{\bar{\nu}_e}$	$\frac{\text{total}}{\nu_x}$	$\frac{\text{total}}{\nu_e}$	$\frac{\text{total}}{\bar{\nu}_e}$	$\frac{\text{total}}{\nu_x}$
PNS, equipart	5.2	6.6	1.5	6.1	6.6	1.5	7.8	6.6	1.4	6.1	5.2	1.6	7.8	5.2	1.5
PNS, from [17]	6.0	6.0	1.5	6.0	6.0	1.5	6.0	6.0	1.5	6.0	6.0	1.5	6.0	6.0	1.5
$\dot{m} = 1.0$ from [14]	1600	7.6	1.2	4.0	7.6	1.6	1.8	7.6	3.2	4.0	1600	1.3	1.8	1600	2.3
$\dot{m} = 0.1$ from [14]	78	3.0	1.5	6.5	3.0	2.0	3.0	3.0	3.0	6.5	78	1.2	3.0	78	1.5
$\dot{m} = 0.01$ from[14]	41	2.7	1.7	7.6	2.7	2.0	3.8	2.7	2.8	7.6	41	1.2	3.8	41	1.4

TABLE I: Ratios of energy fluxes for various accretion disk models and oscillation scenarios as compared with the PNS. The PNS is calculated for the case of equipartition of energy between neutrino species, and for the luminosity ratios ratios of Fig. 2. The quantity ν_x refers to the sum of the ν_μ, ν_τ and $\bar{\nu}_\mu$ and $\bar{\nu}_\tau$ luminosities. Five oscillation scenarios are shown. H means that either neutrinos or antineutrinos, depending on the hierarchy, proceed adiabatically through the higher density resonance (i.e. $P_{hop} = 0$). LA means that neutrinos proceed adiabatically through the lower density resonance, while LNA means that neutrino pass nonadiabatically through the lower density resonance (i.e. $P_{hop} = 1$).

		$\dot{m}$				$\dot{m}$				$\dot{m}$				$\dot{m}$				$\dot{m}$		
	PNS	1.0	0.1	0.01	PNS	1.0	0.1	0.01	PNS	1.0	0.1	0.01	PNS	1.0	0.1	0.01	PNS	1.0	0.1	0.01
SuperK																				
$\bar{\nu}_e + p \rightarrow n + e^+$	7000	2800	1400	50	7000	2800	1400	50	7000	2800	1400	50	10000	10	50	2	10000	10	50	2
$\nu + ^{16}0$	30	20	3.0	0.3	30	20	3.0	0.3	30	20	3.0	0.3	30	20	3.0	0.3	30	20	3.0	0.3
SNO																				
$\nu_e + d \rightarrow p + p + e^-$	170	0.2	0.8	0.04	130	80	10	0.2	80	180	20	0.4	130	80	10	0.2	80	180	20	0.4
$\bar{\nu}_e + d \rightarrow n + n + e^+$	70	30	0.2	0.4	70	30	15	0.4	70	30	6	0.4	100	0.1	0.5	0.02	100	0.1	0.5	0.02
$\nu + d \rightarrow p + n + \nu$	330	140	30	0.7	330	140	30	0.7	330	140	30	0.7	330	140	30	0.7	330	140	30	0.7
KamLAND																				
$\bar{\nu}_e + p \rightarrow n + e^+$	280	110	50	2	280	110	50	2	280	110	50	2	380	0.5	3	0.1	380	0.5	3	0.1
$\nu + p \rightarrow \nu + p$	500	200	44	1	500	200	44	1	500	200	44	1	500	200	44	1	500	200	44	1
OMNIS																				
$\nu_e + \text{Pb} \rightarrow e^- + n + \text{Bi}$	210	0.1	0.9	0.2	150	90	10	0.1	80	190	30	0.3	150	90	10	0.1	80	190	30	0.2
$\nu + \text{Pb} \rightarrow \nu + \text{Pb} + n$	40	16	4	0.04	40	16	4	0.04	40	16	4	0.04	40	16	4	0.04	40	16	4	0.04

TABLE II: Integrated counts in various detectors. The columns represent the same oscillation scenarios as in Table I. All accretion disk rates may be scaled by $(M/M_\odot)$ where M is the mass of material processed by the disk. OMNIS rates are quoted for 1kt of lead perchlorate only. More detailed discussion of count rates for the PNS are in, e.g. [11, 20, 21, 22].